

Raising Schrödinger’s cat with a levitated nanodiamond through spin-opto-mechanical coupling

Zhang-qi Yin,^{1,*} Tongcang Li,² Xiang Zhang,² and L. M. Duan^{1,3}

¹*The Center for Quantum Information, Institute for Interdisciplinary Information Sciences, Tsinghua University, Beijing 100084, P. R. China*

²*NSF Nanoscale Science and Engineering Center, 3112 Etcheverry Hall, University of California, Berkeley, California 94720, USA*

³*Department of Physics, University of Michigan, Ann Arbor, Michigan 48109, USA*

(Dated: September 29, 2018)

We propose a method to generate and detect Schrödinger’s cat state and superposition of arbitrary Fock states for the oscillational mode of an optically levitated nanocrystal diamond. The nonlinear interaction required for generation of non-Gaussian quantum states is enabled through the spin-opto-mechanical coupling with a built-in nitrogen-vacancy center inside the nanodiamond. The proposed method allows raising of Schrödinger’s cat states from single atoms to much larger objects with millions of atoms and observation of the associated spatial quantum interference of the mesoscopic nanodiamond under reasonable experimental conditions.

Creating Schrödinger’s cat states with massive objects is one of the most challenging and attractive goals in macroscopic quantum mechanics [1–4]. It provides potential opportunities to experimentally test different wave-function collapse models [2], including gravity-induced state reduction [5], which is a manifestation of the apparent conflict between general relativity and quantum mechanics. Quantum superpositions and interferences have been realized with electrons, neutrons, atoms, and complex molecules with several hundred atoms [6]. Among different optomechanical systems [7–10], optically levitated dielectric particles in vacuum [11–21] are particularly promising for creating superposition states with the largest *macroscopicity* (as defined in Ref. [4]). Due to the absence of the mechanical contact in this system, the decoherence [22] can be negligible and the oscillation frequency is fully tunable. Once cooled to the quantum regime, optically trapped nanoparticles in vacuum will be ultra-sensitive detectors [23–25], and can be even used to study self-assembly of the nanoparticles in vacuum [26, 27]. To generate spatial quantum superpositions and other non-Gaussian states with an optical cavity, however, requires a very strong quadratic coupling [21, 28]. This is a very demanding requirement. To enhance the quadratic coupling, Romero-Isart *et al.* [21] proposed to prepare spatial quantum superpositions of nanoparticles with two inter-connected high-finesse optical cavities: one cavity for cooling, and the other cavity for preparing the superposition state with a squared position measurement when the nanoparticle falls through it.

In this paper, we propose a scheme to generate and detect arbitrary Fock states and Schrödinger’s cat states for the center-of-mass oscillation of an optically trapped nanocrystal diamond using the induced spin-opto-mechanical coupling. The nanodiamond has built-in nitrogen-vacancy (NV) centers, and electron spins associated with diamond NV centers make good qubits for

quantum information processing as they have nice coherence properties even at room temperature [29]. Nanodiamonds with NV centers have been recently trapped by optical tweezers in fluid [30–32], and similar technologies can be used to optically trap them in vacuum [16]. With assistance of a strong magnetic field gradient from a nearby magnetic tip, strong coupling between the NV spin and the mechanical oscillation of the nanodiamond can be achieved. Using this coupling, we show how to generate entanglement between the NV spin states and distinguishable positions of the nanodiamond and prepare Schrödinger’s cat states for the nanodiamond with big quantum superpositions at distinct locations. We also show how to generate arbitrary Fock states and their superpositions for the nanodiamond. The generated Schrödinger’s cat states and other mesoscopic quantum superposition states can be detected through different spatial interference patterns of the nanodiamond.

The proposed setup. As shown in Fig. 1a, we consider a nano-diamond trapped by an optical tweezer in a high-Q cavity in vacuum. Therefore, the mechanical motion of the nanodiamond couples with the cavity mode. The trap is located in a place that the cavity mode has the maximum gradient. Near the NV center, there is a magnet tip [33], which induces a strong magnetic field gradient. The magnetic gradient couples the mechanical motion and the electron spin. There is also a microwave source to control the spin of the NV center inside the nanodiamond. The main feature of our scheme is that spin (microwave), mechanical mode (radio frequency), and optical cavity mode (optical frequency) are coupled with each other. As the nanodiamond is optically trapped in the vacuum, the coherence time of the mechanical mode for its center-of-mass motion is long [11–15]. The frequency of the optical trap can be quickly tuned through control of the laser intensity. This feature is important as we can cool the mechanical mode to the ground state in a strong trap and prepare large quantum

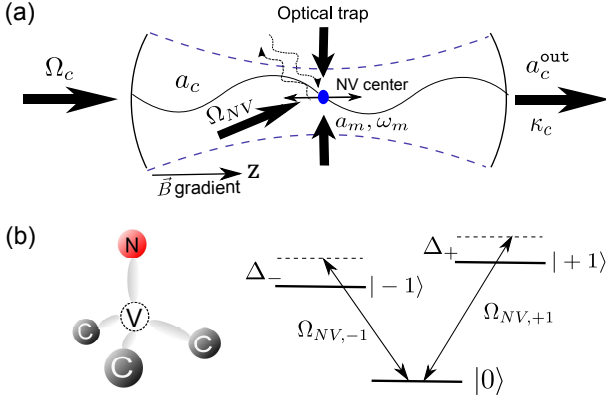


FIG. 1: (Color online) (a) A nanodiamond with a NV center is trapped by an optical tweezer in an optical cavity in vacuum. Near the optical tweezer, there is a magnetic tip (not shown) which induces a strong magnetic gradient. A microwave source is used to control the spin of the NV center, which can be initialized with an optical pump. (b) The atomic structure of a NV center in diamond is shown in the left. The level diagram of the driven NV center in the electronic ground state is shown in the right.

superposition states of the nanodiamond in a weak trap by a quench of the trap frequency.

The atomic structure and the level configuration of the NV centers is shown in Fig.1b. The Hamiltonian of the system is $H = H_{NV} + H_c + H_m + H_{mc} + H_{NVm} + H_{drive}$. Here $H_{NV} = \hbar(\omega_{+1}|+1\rangle\langle+1| + \omega_{-1}|-1\rangle\langle-1|)$ is the Hamiltonian of the NV center electron spin. We set the level $|0\rangle$ as the reference level. $H_m = \hbar\omega_m a_m^\dagger a_m$ is the Hamiltonian of the mechanical mode for the center-of-mass motion of the nanodiamond. $H_c = \hbar\omega_c a_c^\dagger a_c$ is the Hamiltonian of the cavity mode. $H_{mc} = \hbar g a_c^\dagger a_c (a_m + a_m^\dagger)$ is the interaction Hamiltonian between the mechanical mode and the cavity mode, where $g = a_0 \partial U(z) / \partial z$ is the coupling strength, $a_0 = \sqrt{\hbar / 2m\omega_m}$ is the zero-point fluctuation for the mechanical mode a_m , and $U(z)$ characterizes the cavity mode induced potential for a nanodiamond. $H_{NVm} = \hbar\lambda S_z (a_m + a_m^\dagger)$ is the interaction Hamiltonian between the NV center and the mechanical mode [34, 35]. Here, $S_z = |+1\rangle\langle+1| - |-1\rangle\langle-1|$, and $\lambda = g_s \mu_B G_m a_0 / \hbar$ characterizes the spin-phonon coupling strength, where $g_s \simeq 2$ is the Landé g-factor, μ_B is the Bohr magneton, G_m is the magnetic field gradient along the NV center axis. $H_{drive} = \hbar(\Omega_c e^{-i\omega_L t} a + h.c.) / 2 + \hbar(\Omega_{NV,+1} e^{i\omega_L t} |0\rangle\langle+1| + \Omega_{NV,-1} e^{i\omega_L t} |0\rangle\langle-1| + h.c.) / 2$ characterizes the optical driving on the cavity mode and the microwave driving on the NV center spin. We denote $\Delta_c = \omega_L - \omega_c$ as the detuning between the driving laser and the cavity mode, and $\Delta_\pm = \omega_{l\pm} - \omega_{\pm 1}$ as the detunings between the driving microwave and the NV center spin transitions. We assume that the frequency of the cavity mode is far away from the optical transitions of the NV center and therefore there is no direct spin-photon coupling.

Preparation and detection of Fock states. In order to prepare the Fock states, we first cool the mechanical mode to the ground state. The NV center is initially set to the state $|0\rangle$, which is decoupled from the mechanical mode. Initialization and single shot detection of the NV center spin have been well accomplished experimentally [36]. The ground state cooling for the center-of-mass oscillation of the nanodiamond can be achieved with the cavity-assisted cooling as has been demonstrated for other systems [9]. With a red-detuned driving laser for the cavity mode with the detuning $\Delta_c = -\omega_m$, the steady state of the cavity is a coherent state $|\alpha_c\rangle$ with $\alpha_c = i\Omega_c / (2i\Delta_c - \kappa_c)$. In the region of strong trapping with $\omega_m \gg \kappa$, the mechanical mode can be cooled down to the ground state with the final thermal phonon number $n_{mf} = (\kappa / 4\omega_m)^2 \ll 1$. The heating of the mechanical mode is negligible compared with the cooling rate $\Gamma = g^2 |\alpha_c|^2 / \kappa$ as the Q -factor for center-of-mass oscillation of an optically trapped object could be higher than 10^{10} in a high vacuum [11]. Note that the center-mass oscillation is well decoupled from the other phonon (mechanical) modes of the diamond and thus not subject to the intrinsic dissipation of the material and can be cooled to the ground state even if the diamond itself (the other phonon modes) is at room temperature. An alternative way for the ground state cooling of the center-of-mass mode, although not demonstrated yet in experiments, is to use a combination of the optical pumping cooling of the NV spin state and the fast exchange between the spin and the motional excitations [34]. In this case, we do not need any optical cavity, which could further simplify the experimental setup.

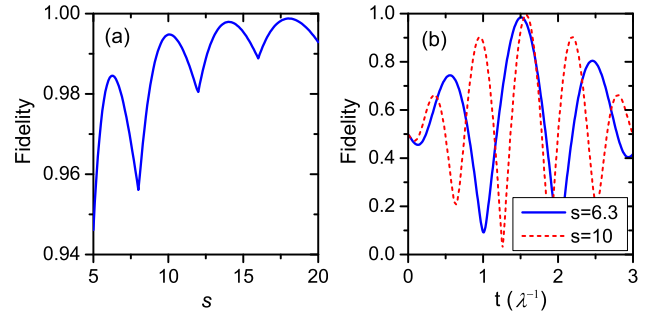


FIG. 2: Fidelity of creating the phonon number superposition state $(|0\rangle_m + i|1\rangle_m) / \sqrt{2}$ by coherent state transfer between the NV spin and the mechanical mode. Fidelities higher than 99% can be achieved. (a) The peak fidelity as a function of the parameter $s = \omega_m / \lambda$. (b) The fidelity as a function of the interaction time for two different parameters ($s = 6.3, 10$).

We assume that the NV center is at a position with zero magnetic field and a large field gradient. With a microwave drive, we have $\Delta_+ = \Delta_- = \Delta$ and $\Omega_{NV,+1} = \Omega_{NV,-1} = \Omega_{NV}$ in Fig. 1. When the detuning $\Delta \gg |\Omega_{NV}|$, we adiabatically eliminate the level $|0\rangle$ and get

the following effective Hamiltonian

$$H_e = \omega_m a_m^\dagger a_m + \Omega \sigma_z + \lambda(\sigma_+ + \sigma_-)(a_m + a_m^\dagger), \quad (1)$$

where $\Omega = |\Omega_{\text{NV}}|^2/4\Delta$, $\sigma_z = |+\rangle\langle+| - |-\rangle\langle-|$, $\sigma_+ = |+\rangle\langle-|$, $\sigma_- = |-\rangle\langle+|$, and we have defined the new basis states $|+\rangle = (|+1\rangle + |-1\rangle)/\sqrt{2}$, $|-\rangle = (|-1\rangle - |+1\rangle)/\sqrt{2}$. In the limit $\lambda \ll \omega_m$, we set $\Omega = \omega_m/2$ and use the rotating wave approximation to get an effective interaction Hamiltonian between mechanical mode and the NV center spin, with the form $H_{JC} = \hbar\lambda\sigma_+ a_m + h.c.$. This represents the standard Jaynes-Cummings(J-C) coupling Hamiltonian. Similarly, if we set $\Omega = -\omega_m/2$, the anti J-C Hamiltonian can be realized with $H_{aJC} = \hbar\lambda\sigma_+ a_m^\dagger + h.c.$.

Arbitrary Fock states and their superpositions can be prepared with a combination of J-C and anti J-C coupling Hamiltonians. For example, to generate the Fock state $|2\rangle_m$, we initialize the state to $|+\rangle|0\rangle_m$, turn on the J-C coupling for a time duration $t_1 = \pi/(2\lambda)$ to get $|-\rangle|1\rangle_m$, and then turn on the anti J-C coupling for a duration $t_2 = t_1/\sqrt{2}$ to get $|+\rangle|2\rangle_m$. The Fock state with arbitrary phonon number n_m can be generated by repeating the above two basic steps, and the interaction time is $t_i = t_1/\sqrt{i}$ for the i th step [37]. Superpositions of different Fock states can also be generated. For instance, if we initialize the state to $(c_0|+\rangle + c_1|-\rangle) \otimes |0\rangle_m/\sqrt{2}$ through a microwave with arbitrary coefficients c_0, c_1 , and turn on the J-C coupling for a duration t_1 , we get the superposition state $|-\rangle \otimes (c_1|0\rangle_m + ic_0|1\rangle_m)/\sqrt{2}$. In Fig. 2a, we plot the fidelity of the mechanical state as a function of the parameter $s = \omega_m/\lambda$ using the full Hamiltonian with rotating wave approximation. The fidelity oscillates with many local maxima and the envelope approaches unity when $s \gg 1$. In practice, we have a very high fidelity already by setting s at the local maxima such as 6.3 or 10.0. Using the optical cavity, the Fock state $|n_m\rangle_m$ of mechanical mode can also be mapped to the corresponding Fock state of the output light field [25].

The effective Hamiltonian for the spin-phonon coupling takes the form $H_{QND} = \hbar\chi\sigma_z a_m^\dagger a_m$ with $\chi = 4\Omega\lambda^2/(4\Omega^2 - \omega_m^2)$ when the detuning $|\Omega - \omega_m/2| \gg \lambda$. The Hamiltonian H_{QND} can be used for a quantum non-demolition measurement(QND) measurement of the phonon number: we prepare the NV center spin in a superposition state $|+\rangle + e^{i\phi}|-\rangle/\sqrt{2}$, and the phase ϕ evolves by $\phi(t) = \phi_0 + 2\chi n_m t$, where $n_m = a_m^\dagger a_m$ denotes the phonon number. Through a measurement of the phase change, one can detect the phonon number. The preparation and detection of the Fock states can all be done within the spin coherence time. Let us estimate the typical parameters. A large magnetic field gradient can be generated by moving the nanodiamond close to a magnetic tip. A large field gradient up to 4×10^7 T/m has been reported in 2006 near the write head of a magnetic disk drive [33]. Here we take the gradient $G = 10^5$ T/m

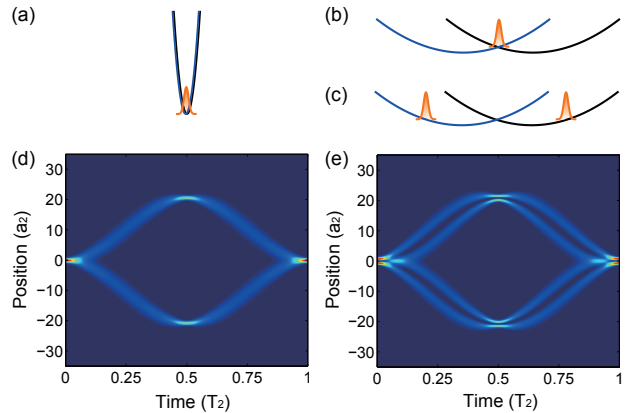


FIG. 3: (a) A nanodiamond with $d = 30$ nm is confined tightly by a 100kHz frequency optical tweezer in a magnetic field with a large gradient $G = 4 \times 10^4$ T/m. Its NV center is prepared in a state $|0\rangle$. (b) The power of the optical tweezer is suddenly reduced to 20kHz, and NV center is changed to a superposition state $(|+1\rangle + |-1\rangle)/\sqrt{2}$, while the magnetic gradient is the same. As a result, the trap centers for different electron spins are separated. (c) The nanodiamond becomes in a spatial superposition state as the state evolves in time. (d) The time evolution of the probability distribution of the nanodiamond after trapping frequency and NV center state is suddenly changed. The mechanical state is initially $|0\rangle_{m,100\text{kHz}}$ in the high frequency trap. $a_2 = \sqrt{\hbar/2m\omega_m/2} = 0.092$ nm, and $T_2 = 50\mu\text{s}$. (e) The mechanical state is initially $|1\rangle_{m,100\text{kHz}}$. Other parameters are the same as those for (d). The spatial separation is maximum after half period of evolution.

and get the coupling $\lambda \simeq 2\pi \times 52$ kHz for a nanodiamond with the diameter $d = 30$ nm in an optical trap with a trapping frequency $\omega_m = 2\pi \times 0.5$ MHz. The Fock states and their superpositions can then be generated with a time scale $1/\lambda$ about a few μs , and the QND detection rate $2|\chi| \sim 2\pi \times 25$ kHz with the detuning $|\Omega - \omega_m/2| \sim 5\lambda$. The NV electron spin dephasing time over 1.8 ms has been observed at room temperature [38], which is long compared with the Fock state preparation time $1/\lambda$ and the detection time $1/(2|\chi|)$.

Generation and detection of large Schrödinger's cat states. To prepare Schrödinger's cat state, we need to generate quantum superposition of the nanodiamond at distinct locations. Without the microwave driving, the spin-mechanical coupling Hamiltonian takes the form

$$H = \hbar\omega_m a_m^\dagger a_m + \hbar\lambda S_z (a_m + a_m^\dagger). \quad (2)$$

The mechanical mode is initialized to the vacuum state $|0\rangle_m$ (or a Fock state $|n_m\rangle$) in a strong trap with the trapping frequency ω_{m0} and the NV center spin is prepared in the state $|0\rangle$. Although the ground state cooling is most effective in a strong trap, to generate large spatial separation of the wave packets it is better to first lower the trap frequency by tuning the laser intensity for the optical trap. While it is possible to lower the trap frequency

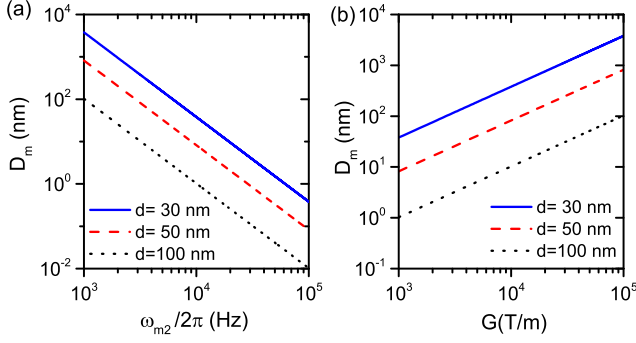


FIG. 4: (a) Maximum spatial separation D_m of the superposition state as a function of trap frequency ω_{m2} when the magnetic gradient is 10^5 T/m. (b) Maximum spatial separation D_m as a function of the magnetic gradient G when the trapping frequency is 1 kHz. Macroscopic superposition states with separation larger than the size of the particle can be achieved with a moderate magnetic gradient.

through an adiabatic sweep to keep the phonon state unchanged, a more effective way is to use a non-adiabatic state-preserving sweep [39], which allows arbitrarily short sweeping time. The trap frequency $\omega_m(t)$ is lowered from ω_{m0} to ω_{m1} with a duration t_f through the following time dependence $\omega_m^2(t) = [\omega_m^2(0)/b^4(t)] - [\dot{b}(t)/b(t)]$, where $b(t) = 6(r-1)s^5 - 15(r-1)s^4 + 10(r-1)s^3 + 1$ with $s = t/t_f$ and $r = \sqrt{\omega_{m0}/\omega_{m1}}$ [39]. The phonon distribution remains unchanged during this sweep. We denote $|n_m\rangle_1$ as the mechanical state in the lower frequency ω_{m1} . We then apply an impulsive microwave pulse to suddenly change the NV spin to the state $(|+1\rangle + |-1\rangle)/\sqrt{2}$ and simultaneously decrease the trap frequency to $\omega_{m2} \leq \omega_{m1}$. The evolution of the system state under the Hamiltonian (2) then automatically split the wave packet for the center-of-mass motion of the nanodiamond (see the illustration in Fig. 3). The splitting attains the maximum at time $T_2/2 = \pi/\omega_{m2}$, where the maximum distance of the two wave packets in the superposition state is $D_m = 8\lambda a_2/\omega_{m2} = 4g_s\mu_B G/(m\omega_{m2}^2)$, where $a_2 = \sqrt{\hbar/2m\omega_{m2}}$. At this moment, the system state is $|\Psi_S\rangle = (|+1\rangle|D_m/2\rangle_{n_m} + |-1\rangle|-D_m/2\rangle_{n_m})/\sqrt{2}$, where $|\pm D_m/2\rangle_{n_m} \equiv (-1)^{a_m^\dagger a_m} \exp[\pm D_m(a_m^\dagger - a_m)/4a_2] |n_m\rangle_1$ is the displaced Fock state (or coherent states when $n_m = 0$). This is just the entangled Schrodinger's cat state. In Fig. 3 (d) and (e), we show the evolution of the splitting of the spatial wave packets for the nanodiamond under the initial vacuum $|0_m\rangle$ or Fock state $|1_m\rangle$. The maximum distance D_m is plotted in Fig. 4 versus trap frequency, magnetic field gradient, and diameter d of the nanodiamond, and superposition states with separation D_m comparable to or larger than the diameter d is achievable under realistic experimental conditions. To transform the entangled cat state $|\Psi_S\rangle$ to the standard cat state $|\psi_\pm\rangle_{n_m} \equiv (|D_m/2\rangle_{n_m} \pm |-D_m/2\rangle_{n_m})/\sqrt{2}$,

we need to apply a disentangling operation to conditionally flip the NV spin using displacement of the diamond as the control qubit. This can be achieved as different displacements of the wavepacket induce relative energy shifts of the spin levels due to the applied magnetic field gradient. As an estimate, for the example we considered in Fig. 5 (with a 30nm-diameter diamond in a 20 kHz trap under a magnetic gradient of 3×10^4 T/m), the spin energy splitting is about 2.4 MHz between the $|+1\rangle|D_m/2\rangle_{n_m}$ and $|-1\rangle|-D_m/2\rangle_{n_m}$ components, which is much larger than the typical transition linewidth (in the order of kHz) of the NV spin. So we can apply first an impulsive microwave pulse to transfer the component state $|+1\rangle|D_m/2\rangle_{n_m}$ to $|0\rangle|D_m/2\rangle_{n_m}$ without affecting $|-1\rangle|-D_m/2\rangle_{n_m}$ and then another pulse to transfer $|-1\rangle|-D_m/2\rangle_{n_m}$ to $\pm|0\rangle|-D_m/2\rangle_{n_m}$. After the two pulses, the spin state gets disentangled and the position of the diamond is prepared in the standard Schrodinger cat state $|\psi_\pm\rangle_{n_m}$.

To detect Schrödinger's cat state, we can turn off the optical trap and let the spatial wave function freely evolve for some time t . The split wave packets will interference just like the Young's double slit experiment. The period of the interference pattern is $\Delta x = 2\pi\hbar t/(mD_m)$. As an estimation of typical parameters, we take $\omega_{m1} = \omega_{m2} = 2\pi \times 20$ kHz, $d = 30$ nm, and magnetic field gradient 3×10^4 T/m. The spin-phonon coupling rate $\lambda \simeq 2\pi \times 77$ kHz and the maximum distance $D_m \simeq 31a_2$. The preparing time of Schrödinger's cat state is about 25 μ s, which is much less than the coherence time of the NV spin. For the time of flight measurement after turn-off of the trap, we see the interference pattern with a period of 47 nm after $t = 10$ ms, as shown in Fig. 5, which is large enough to be spatially resolved [14].

Finally, we briefly mention the source of decoherence for preparation of the Schrodinger cat state. The decoherence of the cat state by photon scattering is negligible during the time-of-flight measurement as the laser is turned off. The main source of decoherence includes background gas collision and black-body radiation. Using the formula in Ref. [21], we estimate that the decoherence rate due to the background gas collision is about 8 Hz under the condition that the vacuum pressure $P \sim 10^{-11}$ Torr and the gas temperature $T_b \sim 4.5$ K. This rate is small compared with the experimental time scale of 10 ms. As the internal temperature T_i of the diamond is typically much higher than the background gas temperature T_b , the black-body radiation is dominated by the thermal photon emission from the diamond. The frequency of the thermal photon is in the order of THz. Compared with the silica sphere considered in [21], the emission rate of THz photons is smaller by about two orders of magnitude for the diamond. Even with T_i at the room temperature, the decoherence rate γ_{bb} due to the thermal photon emission is estimated to be only 3 Hz for our proposed scheme. In addition, with the built-in elec-

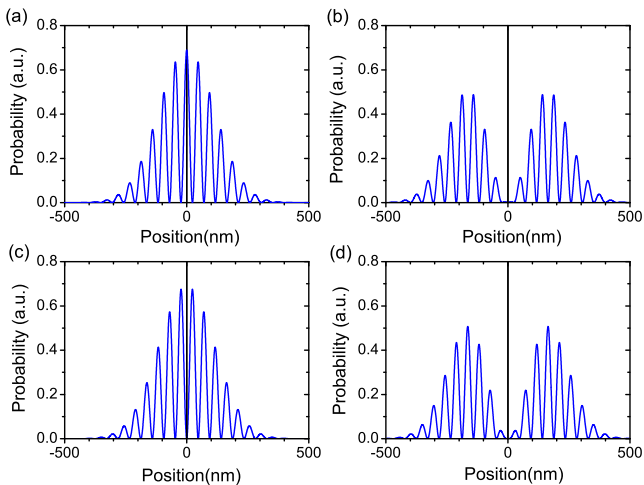


FIG. 5: Spatial interference patterns for a 30 nm nano-diamond after 10 ms of free expansion. The nano-diamond is initially prepared in the vacuum state $|0\rangle_m$ or the 1-phonon state $|1\rangle_m$ of a 20 kHz trap. Then its electron spin is changed to a superposition state, and the wavepacket is split to two spatially distinct states with a magnetic gradient of $3 \times 10^4 \text{T/m}$. The trap is turned off when the separation is maximum. Before the trap is turned off, the center of mass of the nano-diamond is prepared in (a) $|\psi_+\rangle_0$, (b) $|\psi_+\rangle_1$, (c) $|\psi_-\rangle_0$, and (d) $|\psi_-\rangle_1$.

tronic states of the NV center, the internal temperature of the diamond can be reduced through laser cooling [40]. As $\gamma_{bb} \propto T_i^6$, this allows further significant suppression of the decoherence rate.

In summary, we have proposed a scheme to generate Schrödinger's cat state and arbitrary Fock states for the center-of-mass motion of a levitated nanodiamond through the spin-opto-mechanical coupling. Fock states can be detected through measurement of the NV center spin inside the nanodiamond. Schrödinger's cat states lead to characteristic macroscopic interference patterns of the nanodiamond during the time-of-flight, which can be confirmed through position measurement. The same scheme could also apply to other optically levitated nanoparticles with build-in electron spins, such as ^{28}Si nanoparticles with donor spins [41] or nano-crystals doped with rare-earth ions [42]. The proposed scheme opens up the possibility to observe big quantum superpositions for mesoscopic objects under realistic experimental conditions and to test predictions of quantum mechanics in unexplored regions.

We thank Jing-ning Zhang, K. C. Fong, and S. Kheifets for helpful discussion. This work was funded by the NBRPC (973 Program) 2011CBA00300 (2011CBA00301), NNSFC 61033001, 11105136. LMD acknowledge support from the IARPA MUSIQC program, the ARO and the AFOSR MURI program. TL and XZ were supported by NSF Nanoscale Science and Engineering Center (CMMI-0751621). TL and ZQY pro-

posed the project, ZQY and TL did the calculations, all authors contributed in the discussion and writing of the paper.

* yinzhangqi@mail.tsinghua.edu.cn

- [1] K. Hornberger, S. Gerlich, P. Haslinger, S. Nimmrichter, and M. Arndt, *Rev. Mod. Phys.* **84**, 157 (2012).
- [2] A. Bassi, K. Lochan, S. Satin, T. P. Singh, and H. Ulbricht, *Rev. Mod. Phys.* **85**, 471 (2013).
- [3] Yanbei Chen, arXiv:1302.1924 (2013).
- [4] S. Nimmrichter, and K. Hornberger, *Phys. Rev. Lett.* **110**, 160403 (2013)
- [5] R. Penrose, *Gen. Relativ. Gravit.* **28**, 581 (1996).
- [6] C. Davisson and L. H. Germer, *Nature (London)* **119**, 558 (1927); I. Estermann and O. Stern, *Z. Phys.* **61**, 95 (1930); W. Schöllkopf and J. P. Toennies, *Science* **266**, 1345 (1994); M. Kasevich and S. Chu, *Phys. Rev. Lett.* **67**, 181 (1991); C. Monroe *et al.*, *Science* **272**, 1131 (1996); M. Arndt *et al.*, *Nature (London)* **401**, 680 (1999); Gerlich, S. *et al.*, *Nat. Commun.* **2**, 263 (2011).
- [7] I. Wilson-Rae, N. Nooshi, W. Zwerger, and T. J. Kippenberg, *Phys. Rev. Lett.* **99**, 093901 (2007).
- [8] F. Marquardt, J. P. Chen, A. A. Clerk, and S. M. Girvin, *Phys. Rev. Lett.* **99**, 093902 (2007).
- [9] A. D. O'Connell *et al.*, *Nature (London)* **464**, 697 (2010); Jasper Chan *et al.*, *Nature (London)* **478**, 89 (2011); J. D. Teufel *et al.*, *Nature (London)* **475**, 359 (2011).
- [10] M. Aspelmeyer, T. J. Kippenberg, F. Marquardt, arXiv:1303.0733 (2013);
- [11] D. E. Chang *et al.*, *Proc. Natl. Acad. Sci. USA* **107**, 1005 (2010).
- [12] O. Romero-Isart, M. Juan, R. Quidant, and J. Cirac, *New J. Phys.* **12**, 033015 (2010).
- [13] O. Romero-Isart *et al.*, *Phys. Rev. A* **83**, 013803 (2011).
- [14] T. Li, S. Kheifets, D. Medellin, and M. G. Raizen, *Science* **328**, 1673 (2010).
- [15] Tongcang Li, Simon Kheifets, Mark G. Raizen, *Nature Phys.* **7**, 527 (2011).
- [16] Jan Gieseler *et al.*, *Phys. Rev. Lett.* **109**, 103603 (2012).
- [17] T. S. Monteiro *et al.*, *New J. Phys.* **15**, 015001 (2013).
- [18] A. C. Pflanzner, O. Romero-Isart, and J. I. Cirac, *Phys. Rev. A* **86**, 013802 (2012)
- [19] H. K. Cheung, and C. K. Law, *Phys. Rev. A* **86**, 033807 (2012)
- [20] Nikolai Kiesel *et al.*, arXiv:1304.6679
- [21] O. Romero-Isart *et al.*, *Phys. Rev. Lett.* **107**, 020405 (2011); O. Romero-Isart, *Phys. Rev. A* **84**, 052121 (2011)
- [22] Zhang-qi Yin, *Phys. Rev. A* **80**, 033821 (2009)
- [23] A. A. Geraci, S. B. Papp, and J. Kitching, *Phys. Rev. Lett.* **105**, 101101 (2010).
- [24] A. Arvanitaki, A. A. Geraci, *Phys. Rev. Lett.* **110**, 071105 (2013).
- [25] Zhang-qi Yin, Tongcang Li, M. Feng, *Phys. Rev. A* **83**, 013816 (2011).
- [26] W. Lechner, S. J. M. Habraken, N. Kiesel, M. Aspelmeyer, P. Zoller, *Phys. Rev. Lett.* **110**, 143604 (2013).
- [27] S.J.M. Habraken, W. Lechner, P. Zoller, *Phys. Rev. A* **87**, 053808 (2013).
- [28] J. D. Thompson *et al.*, *Nature* **452**, 06715 (2008).
- [29] J. Wrachtrup and F. Jelezko. *Journal of Physics-*

- Condensed Matter **18**, S807 (2006).
- [30] V. R. Horowitz *et al.*, Proc. Natl. Acad. Sci. USA, **109**, 13493 (2012)
 - [31] M. Geiselmann *et al.*, Nature Nanotechnology **8**, 175 (2013)
 - [32] Levi P. Neukirch *et al.*, arXiv:1305.1515.
 - [33] C. Tsang *et al.*, 2006 IEEE Trans. Magn. **42**, 145 (2006).
 - [34] P. Rabl *et al.*, Phys. Rev. B **79**, 041302(R) (2009).
 - [35] S. Kolkowitz *et al.*, Science **335**, 1603 (2012).
 - [36] L. Robledo, L. Childress, H. Bernien, B. Hensen, P. F. A. Alkemade, R. Hanson. Nature **477**, 574 (2011)
 - [37] D. Meekhof *et al.*, Phys. Rev. Lett. **76**, 1796 (1996).
 - [38] G. Balasubramanian and *et al.*, Nat. Mater. **8**, 383 (2009).
 - [39] Xi Chen *et al.*, Phys. Rev. Lett. **104**, 063002 (2010).
 - [40] Denis V. Seletskiy *et al.*, Nature Photon. **4**, 161 (2010); Jun Zhang *et al.* Nature(London) **493**, 504 (2013)
 - [41] M. Steger *et al.*, Science **336**, 1280 (2012).
 - [42] W. Tittel *et al.*, Laser & Photon. Rev. **4**, 244, (2010).